Electronic Supplementary Material (ESI) for Chemical Communications

Supporting Information

A Homochiral Metal-Organic Framework Membrane for Enantioselective Separation

Wenjin Wang,[a,‡] Xueliang Dong,[a,‡] Jiangpu Nan,[a] Wanqin Jin,[a,*] Zhongqiao Hu,[b] Yifei Chen,[b] Jianwen Jiang[b]

[a] State Key Laboratory of Materials-Oriented Chemical Engineering, Nanjing University of Technology, 5 Xinmofan Road, Nanjing 210009, P. R. China.

[b] Department of Chemical and Biomolecular Engineering, National University of Singapore, 4 Eng. Drive 4, Singapore 117576, Singapore.

[‡] These authors contributed equally to this work.

* E-mail: wqjin@njut.edu.cn

1. Experimental details

1.1 Preparation of Zn-BLD crystal

A mixture of $Zn(NO_3)_2 \cdot 6H_2O$ (0.9 g), L-lactic acid (L-H_2lac, 98 %, Alfa Aesar) (0.147 g), 1,4-benzenedicarboxylic acid (H_2BDC, 98 %, Sigma-Aldrich) (0.249 g) and dimethylformamide (DMF) (30 ml) was stirred for 30 minutes to form an homogeneous solution. The solution was then placed in an autoclave (45 ml) and maintained at 110 °C for 24 h. After cooling, the solution was centrifuged. Zn-BLD crystals were obtained after the precipitates were washed with DMF and dried in vacuo at 90 °C.

1.2 Preparation of support

ZnO powders (particle size of ca. 1 mm) were uniaxially pressed at 200 MPa to prepare disks with the diameter of 28 mm and thickness of 2 mm. The disks were then sintered at 620 °C for 2 h to form porous support with the normal pore size of ca. 100 nm and the porosity of about 34 %. One side of the support was polished by SiC sandpaper, washed in deionized water, and dried before being used for the growth of MOF membrane.

1.3 Preparation of Zn-LBD membrane

The homochiral Zn-LBD membrane was prepared on ZnO support by the RS method.[1] A typical synthesis procedure contained two processes. Seeding process: H_2BDC (0.0156 g), L-H_2lac (0.0092 g), and DMF (30 ml) were mixed and stirred vigorously for 30 minutes. A ZnO support was placed, with the smooth surface down, in a Teflon lined stainless steel autoclave (45 ml) with the solution mixture. The autoclave was heated at 110 °C for 12 h in an oven and then cooled down to room temperature. The support with homochiral Zn-LBD seed layer on the surface was washed with DMF and dried at 100 °C for 2 h. Secondary growth: the seeded ZnO support was placed into the precursor solution, with a composition of $Zn(NO_3)_2 \cdot 6H_2O$ (0.36 g), L-H_2lac (0.0294 g), H_2BDC (0.0498 g) and DMF (30 ml). Again, the autoclave including the seeded support and precursor solution was heated at 110 °C for 12 h. After cooling, the membrane was washed with DMF and vacuum dried at 90 °C for 6 h.

1.4 Characterizations

The crystal phases of samples were determined by X-ray diffraction (XRD) with Cu Ka radiation (Bruker, model D8 Advance). Diffraction patterns were collected at

room temperature in the range of $5° \leq 2\theta \leq 50°$ with a step width of 0.05° and a scan rate of 0.2 s per step.

The morphologies of membrane and support were examined by scanning electron microscopy (SEM) (FEI, model QUANTA-200). The working parameters of the SEM are: high voltage (HV) 25-30 kV, work distance (WD) 8-10 mm and spot 3.0.

Single-gas permeation experiments were performed on the permeation setup as reported in our previous work.[1] The permeation of small gas molecule (N_2) was measured at room temperature (25 °C) through the homochiral Zn-LBD membrane and support. The feed side was regulated at different pressures and the permeate side was open to atmosphere. The penetrated gas flow rate was measured by a soap film flowmeter. The results are shown in Fig. S1.

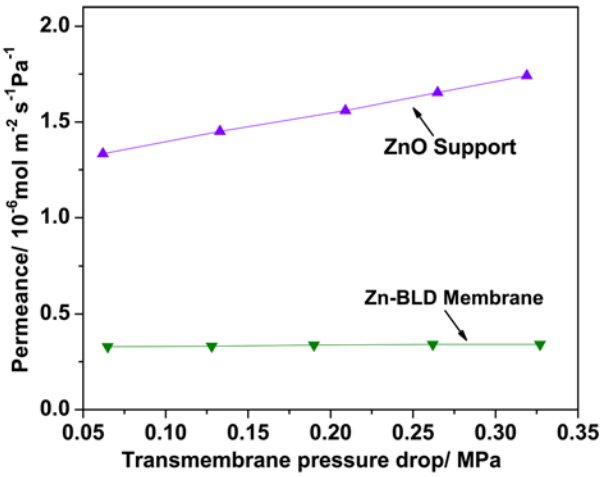

Fig. S1. Permeance of nitrogen through zinc oxide support and homochiral Zn-LBD membrane at different trans-membrane pressure drops.

The concentrations of the enantiomers were analyzed with a high-performance liquid chromatography (HPLC) system (Agilent 1200 Series) equipped with a diode array detector (DAD) and an autosampler. Chromatographic separations were performed at 35 °C using a CHIRALPAK OD-H column (5 μm, 4.6 mm × 250 mm). The analyses were performed by a UV detector at 210 nm using a mobile phase consisting of 80% *n*-Hexane, 20% isopropyl alcohol and a small amount diethylamine at a flow rate of 1 mL·min^{-1}. The injected sample volume was 2 μL.

The enantiomeric excess (*e.e.*) was determined from the peak areas of their two enantiomers, *S*-isomer (A_S) and *R*-isomer (A_R).

$$e.e.(\%) = 100 \times \frac{|A_{R/S} - A_{S/R}|}{A_R + A_S} \qquad \text{(S1)}$$

The permeation flux of the Zn-LBD membrane can be written as

$$flux = \frac{n}{A \cdot t} \qquad \text{(S2)}$$

where n is the permeated *R*- and *S*-MPS (mol), A and t refer to the effective membrane area (m^2) and the permeation time (s), respectively.

1.5. Enantioselective sorption

Racemic MPSs (0.1505 g, 1.073 mmol) was dissolved in CH_2Cl_2 (15 mL), and the partially evacuated Zn-LBD (heated at 90 ºC for 3 h in vacuo before use, 300 mg, 1.275 mmol of zinc atoms) was added to the solution. The XRD diffraction pattern of the used Zn-BLD crystals is shown in Fig. 2a2. After stirring for 16 h at room temperature, the crystalline adsorbent was collected by filtration and flushed with hexane (7.5 mL), by which the adsorbed compounds would not be washed out. The adsorbed MPS was extracted with methanol (75 mL). After stirring for 3 h at room temperature, the extract liquor was collected by filtration. Rotary steaming process was applied to remove the solvent. The resulting MPS was dissolve in *n*-hexane and measured by HPLC. The results are shown in Fig. S2.

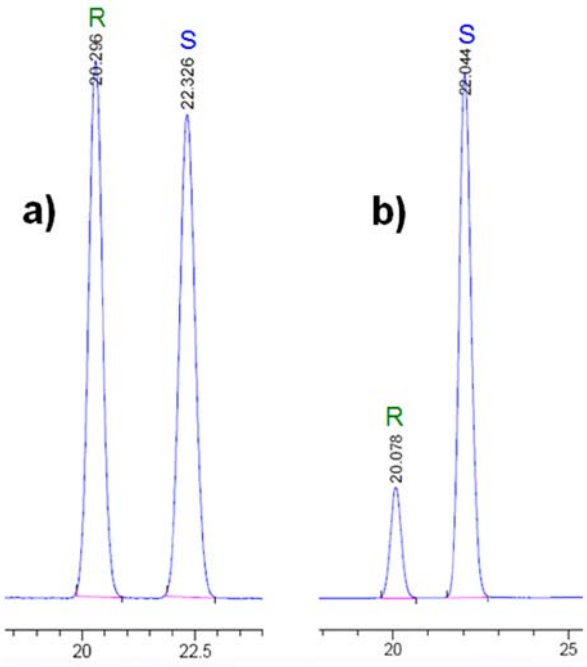

Fig. S2. HPLC data of the concentrations of R-/S-MPS enantiomers before (a) and after (b) adsorption separation.

1.6 Chiral separation experiments

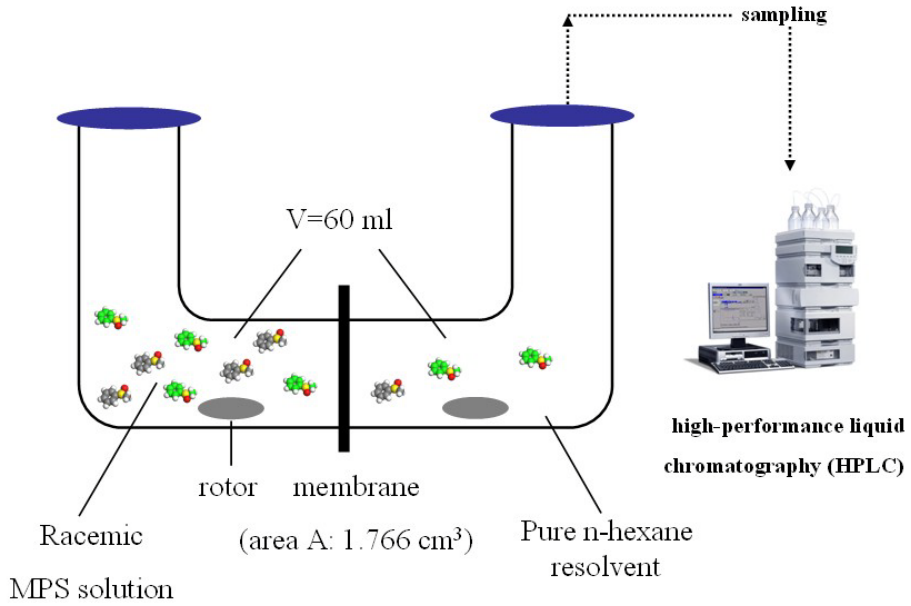

Fig. S3. Schematic diagram of the side-by-side diffusion cell used for the measurement of chiral separation performance of Zn-LBD membrane at 25 ^{o}C.

Fig. S3 shows the schematic diagram of the chiral separation equipment. Two chambers were connected with clamp serve as the dialyzers. A MOF membrane was placed between the two chambers and the fluororubber gaskets were used to seal the connection. The feed side and the permeate side were continuously stirred by magnetic stirring apparatus. Racemic MPSs dissolved in *n*-hexane solvent were introduced to the feed side, while the pure *n*-hexane solvent was used at the acceptor side.

2. Simulation details and results

Atomistic simulation was performed to provide microscopic mechanism into the chiral separation of *R*-/*S*-MPS in the homochiral Zn-BLD membrane. As illustrated in Fig. S4, the simulation system consisted of a supercell (6 × 5 × 3) for Zn-BLD with dimensions of 6.179 nm × 5.912 nm × 6.112 nm. Zn-BLD structure was adopted from the experimentally determined crystallographic data. A racemic mixture of 20 *R*-MPS and 20 *S*-MPS molecules were randomly added into the MOF channels, and the system was solvated by 200 *n*-hexane molecules.

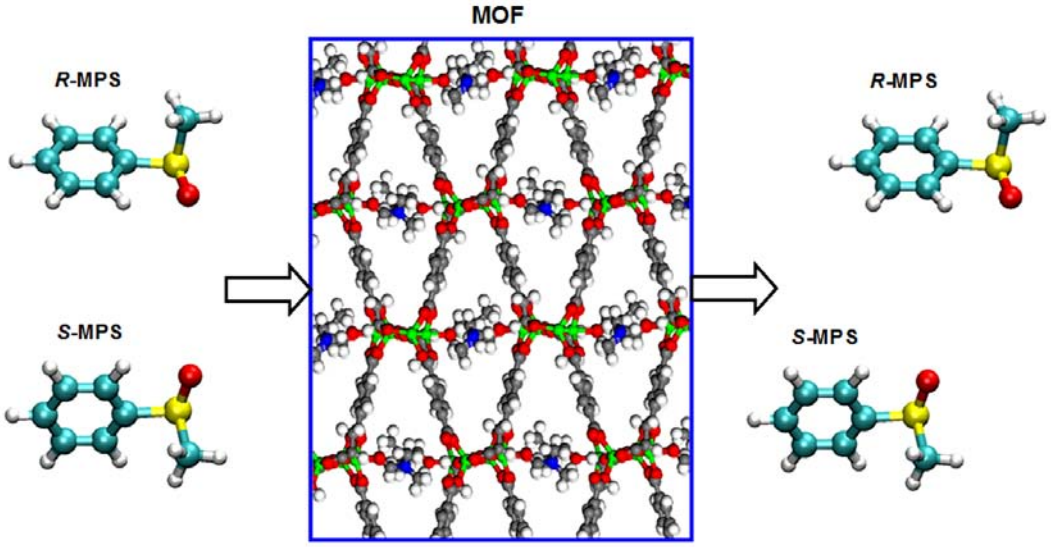

Fig. S4. Schematic illustration for the chiral separation of R-/S-MPS through the homochiral MOF. The R-/S-MPS are shown in the ball-stick mode (C, cyan; O, red; S, orange; H, white). The MOF is shown on the YZ plane (Zn, green; C, grey; O, red; N, blue; H, white). The solvent (n-hexane) molecules are not shown for clarity.

The *R*-/*S*-MPS and *n*-hexane were represented by the Amber force field,[2] in which the interaction has bonded U_{bonded} and non-bonded $U_{\text{nonbonded}}$ terms.

$$U_{\text{total}} = U_{\text{bonded}} + U_{\text{nonbonded}} \quad \text{(S3)}$$

The U_{bonded} term includes stretching, bending, and proper and improper torsional potentials

$$U_{\text{bonded}} = U_{\text{stretching}} + U_{\text{bending}} + U_{\text{proper}} + U_{\text{improper}} \quad \text{(S4)}$$

$$U_{\text{stretching}} = \frac{1}{2} k_b \left(b_{ij} - b_{ij}^0 \right)^2 \quad \text{(S5)}$$

$$U_{\text{bending}} = \frac{1}{2} k_\theta \left(\theta_{ijk} - \theta_{ijk}^0 \right)^2 \quad \text{(S6)}$$

$$U_{\text{proper}} = k_{\phi}\left[1+\cos(m\phi_{ijkl}-\phi^{0}_{ijkl})\right] \quad \text{(S7)}$$

$$U_{\text{improper}} = k_{\xi}\left[1+\cos(m\xi_{ijkl}-\xi^{0}_{ijkl})\right] \quad \text{(S8)}$$

where k_b, k_θ, k_ϕ and k_ξ are the force constants of stretching, bending, and proper and improper torsional potentials, respectively; b_{ij}, θ_{ijk}, ϕ_{ijkl} and ξ_{ijkl} are bond distance, angle, proper and improper dihedral angle, respectively; b^0_{ij}, θ^0_{ijk}, ϕ^0_{ijkl} and ξ^0_{ijkl} are the equilibrium values; m is the multiplicity. The $U_{\text{nonbonded}}$ term includes Lennard-Jones (LJ) and Coulombic potentials

$$U_{\text{nonbonded}} = U_{\text{LJ}} + U_{\text{Coulombic}} \quad \text{(S9)}$$

$$U_{\text{LJ}} = 4\varepsilon_{ij}\left[\left(\frac{\sigma_{ij}}{r_{ij}}\right)^{12}-\left(\frac{\sigma_{ij}}{r_{ij}}\right)^{6}\right] \quad \text{(S10)}$$

$$U_{\text{Coulombic}} = \frac{q_i q_j}{4\pi\varepsilon_0 r_{ij}} \quad \text{(S11)}$$

where σ_{ij} and ε_{ij} are collision diameter and well depth, respectively; q_i is atomic charge of atom i, and $\varepsilon_0 = 8.8542 \times 10^{-12}$ C^2 N^{-1} m^{-2} is vacuum permittivity.

The flexibility of Zn-BLD was taken into account in simulation. The bonded potential parameters for organic linkers were mimicked by the Amber force field;[2] for metal-involved bonds, the parameters were adjusted to reproduce the experimental lattice constants of Zn-BLD. The atomic charges were calculated by density-functional theory (DFT) using a cluster approach. The DFT calculation used the Becke exchange plus Lee-Yang-Parr functional and was carried out with Gaussian 03 package.[3] The 6-31G(d) basis set was used for all atoms except Zn atoms, for which LANL2DZ basis set was used. By fitting the electrostatic potentials produced from the DFT calculation, the atomic charges were estimated.

Gromacs v4.5.3 package[4] was used to perform the simulation with periodic boundary conditions exerted in all three dimensions. The system was initially subject to energy minimization using the steepest descent method with a maximum step size of 0.01 nm and a force tolerance of 10 kJ mol^{-1} nm^{-1}. Then a non-equilibrium molecular dynamics simulation was carried out, as applied in our recent studies for the separation of amino acids and chiral phenylglycines in protein crystals.[5,6] The

velocities were assigned according to the Maxwell-Boltzmann distribution at 300 K. The temperature was controlled at 300 K by the velocity-rescaled Berendsen thermostat[7] with a relaxation time of 0.1 ps. The LJ interactions were evaluated with a cutoff of 1.4 nm and the Coulombic interactions were evaluated using particle-mesh Ewald method with a grid spacing of 0.12 nm and a fourth-order interpolation. An external acceleration of 2 nm ps^{-2} was exerted on solvent molecules and thus *R*-/*S*-MPS molecules were dragged to move. The total simulation duration was 12 ns with a time step of 0.5 fs, and the trajectory was saved every 1 ps. The potential energy of the system and the drift velocities of solvent and solutes were tracked during simulation. A steady state was found to reach in less than 2 ns, thus the final 10 ns trajectory was used for analysis.

The simulated results are shown in Fig. S5.

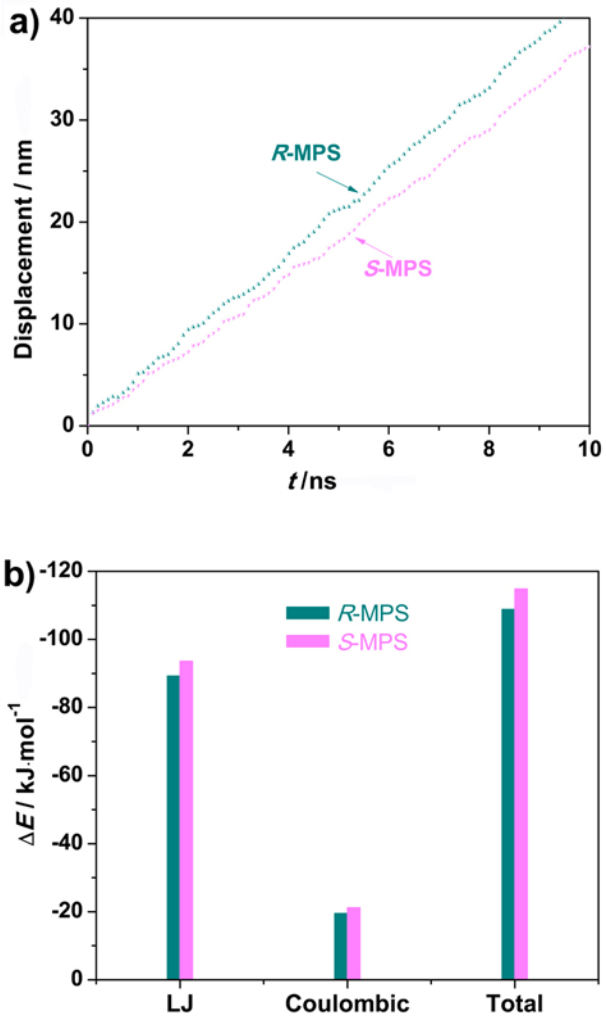

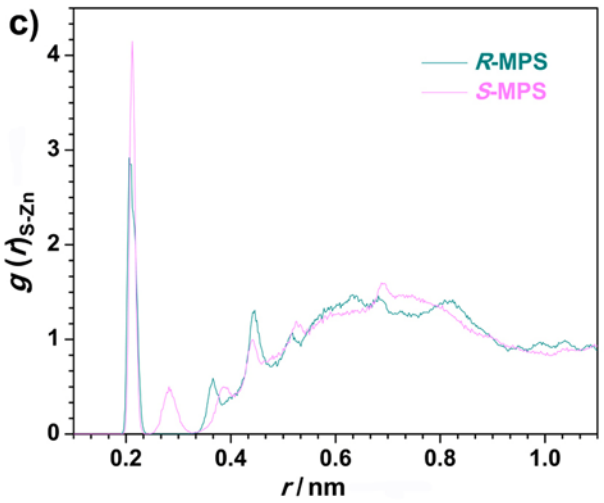

Fig. S5. (a) Displacements of R-/S-MPS in the membrane as a function of simulation duration; (b) Interaction energies of R-/S-MPS with Zn-BLD; (c) Radial distribution functions between sulfur atoms in R-/S-MPS and zinc atoms in Zn-BLD.

References

[1] Y. X. Hu, X. L. Dong, J. P. Nan, W. Q. Jin, X. M. Ren, N. P. Xu, Y. M. Lee, Chem. Commun. **2011**, *47*, 737.

[2] W. D. Cornell, P. Cieplak, C. I. Bayly, I. R. Gould, K. M. Merz, D. M. Ferguson, D. C. Spellmeyer, T. Fox, J. W. Caldwell, P. A. Kollman, *J. Am. Chem. Soc.* **1995,** *117*, 5179.

[3] M. J. Frisch, G. W. Trucks, H. B. Schlegel, G. E. Scuseria, M. A. Robb, J. R. Cheeseman, V. G. Zakrzewski, J. A. Montgomery, R. E. Stratmann, J. C. Burant, S. Dapprich, J. M. Millam, A. D. Daniels, K. N. Kudin, M. C. Strain, O. Farkas, J. Tomasi, V. Barone, M. Cossi, R. Cammi, B. Mennucci, C. Pomelli, C. Adamo, S. Clifford, J. Ochterski, G. A. Petersson, P. Y. Ayala, Q. Cui, K. Morokuma, D. K. Malick, A. D. Rabuck, K. Raghavachari, J. B. Foresman, J. Cioslowski, J. V. Ortiz, B. B. Stefanov, G. Liu, A. Liashenko, P. Piskorz, I. Komaromi, R. Gomperts, R. L. Martin, D. J. Fox, T. Keith, M. A. Al-Laham, C. Y. Peng, A. Nanayakkara, C. Gonzalez, M. Challacombe, P. M. W. Gill, B. G. Johnson, W. Chen, M. W. Wong, J. L. Andres, M. Head-Gordon, E. S. Replogle, J. A. Pople, *Gaussian 03*. Revision D.01 ed.; Gaussian, Inc.: Wallingford CT, **2004**.

[4] D. van der Spoel, E. Lindahl, B. Hess, G. Groenhof, A. E. Mark, H. J. C. Berendsen, *J. Comput. Chem.* **2005,** *26*, 1701.

[5] Z. Q. Hu, J. W. Jiang, *J. Chromatogr. A* **2009,** *1216*, 5122.

[6] Z. Q. Hu, J. W. Jiang, *J. Phys. Chem. B* **2009,** *113*, 15851.

[7] G. Bussi, D. Donadio, M. Parrinello, *J. Chem. Phys.* **2007,** *126*, 014101.